Available online at www.sciencedirect.com
ScienceDirect
Genomics 88 (2006) 468–479
GENOMICS
www.elsevier.com/locate/ygeno

Genomic profiling of cortical neurons following exposure to β-amyloid

Sabrina Paratore [a], Rosalba Parenti [b], Antonietta Torrisi [a], Agata Copani [c], Federico Cicirata [b], Sebastiano Cavallaro [a,*]

[a] Functional Genomics Center, Institute of Neurological Sciences, Italian National Research Council
[b] Department of Physiological Sciences, University of Catania, 95123 Catania, Italy
[c] Department of Pharmaceutical Sciences, University of Catania, 95123 Catania, Italy

Received 12 October 2005; accepted 16 June 2006
Available online 14 August 2006

Abstract

In vitro and in vivo studies have shown that β-amyloid peptide induces neuronal cell death. To explore the molecular basis underlying β-amyloid-induced toxicity, we analyzed gene expression profiles of cultured rat cortical neurons treated for 24 and 48 h with synthetic β-amyloid peptide. From the 8740 genes interrogated by oligonucleotide microarray analysis, 241 genes were found to be differentially expressed and segregated into distinct clusters. Functional clustering based on gene ontologies showed coordinated expression of genes with common biological functions and metabolic pathways. The comparison with genes differentially expressed in cerebellar granule neurons following serum and potassium deprivation indicates the existence of common regulatory mechanisms underlying neuronal cell death. Our results offer a genomic view of the changes that accompany β-amyloid-induced neurodegeneration.

Keywords: Alzheimer disease; Cell death; Neuronal; Genomics; Microarray; Rat

During normal nervous system development, physiologically appropriate neuronal loss contributes to a sculpting process that removes approximately one-half of all neurons born during neurogenesis [1]. Neuronal loss subsequent to this developmental window is physiologically inappropriate for most systems and can contribute to neurological deficits, e.g., neurodegenerative diseases such as Alzheimer disease (AD). Elucidating the molecular mechanisms underlying neuronal death hence will contribute to our understanding of basic developmental biology and human neuropathology.

Changes in the generation or degradation of the β-amyloid peptide (Aβ) are considered the triggering molecular events in the pathogenic cascade that leads to neuronal loss in AD. Aβ, in particular, has been shown to induce neuronal cell death in many in vitro and in vivo studies [2–12]. Because Aβ-induced neuronal cell death may be facilitated by altered gene expression and because genes induced by Aβ may be integral to neuropathological changes observed in AD brain, elucidating patterns of gene expression during neuronal death may be critical to our understanding of Aβ-induced neurotoxicity. Although previous studies implicated individual genes or genetic pathways following exposure to Aβ, their collective behavior is mostly unknown.

In view of the broad variety of genes and the cross talk of genetic pathways, gene expression profiles by microarray technology today offer a new dynamic and functional dimension to the exploration of neurodegeneration. In a previous study we used genome-scale screening by oligonucleotide microarrays to characterize the multigenic program underlying degeneration of cerebellar granule neurons following serum and potassium deprivation [13]. In the present study we used a similar approach to investigate gene expression profiles of cultured cortical neurons exposed to Aβ.

Results

To study the neurotoxic effect of Aβ we used enriched neuronal cultures containing less than 5% astrocytes (Fig. 1A).

* Corresponding author. Fax: + 39 095 7122426.
E-mail address: s.cavallaro@isn.cnr.it (S. Cavallaro).

0888-7543/$ - see front matter © 2006 Elsevier Inc. All rights reserved.
doi:10.1016/j.ygeno.2006.06.007

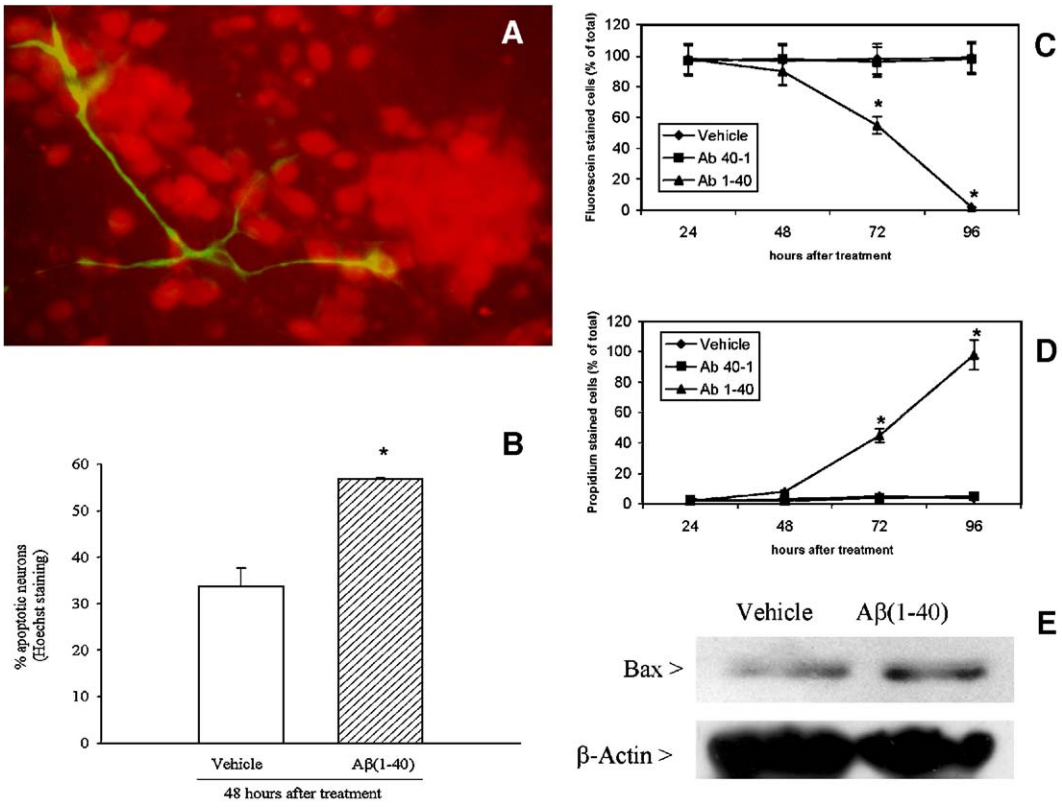

Fig. 1. Primary cultures of rat cortical neurons used to study the neurotoxic effect of Aβ. (A) Double labeling for NeuN and GFAP. To determine the purity of primary cultures of cortical neurons, cells were double labeled for neuron-specific NeuN (Texas red, red signal) and astrocyte-specific GFAP (fluorescein, green signal). (B) Neurons showing typical morphological features of apoptotic degeneration following Aβ 1–40 treatment were analyzed with the nuclear dye Hoechst 33258. (C and D). Viability of neurons assessed by fluorescein/propidium staining. Neurons exposed to 20 μM Aβ 1–40 were not able to sequester fluorescein but showed staining with propidium iodide, an effect consistent with cell degeneration. Exposure of neurons to the reversed Aβ peptide (Aβ 40–1) did not cause any significant degenerative change. In total, 400 cells were counted for each treatment. Data are means±SE. *$p<0.05$ vs control (vehicle and Aβ 40–1-treated neurons). (E) Induction of the apoptosis-related Bax. Western blot analysis was used to assess the expression of the proapoptotic Bax and the structural protein β-actin in neurons treated with Aβ 1–40 for 40 h. (For interpretation of the references to colour in this figure legend, the reader is referred to the web version of this article.)

Some neurons exposed to 20 μM Aβ 1–40 showed typical features of apoptotic degeneration, including chromatin condensation and fragmentation, when analyzed by fluorescence microscopy with the nuclear dye Hoechst 33258 (Fig. 1B). A significant reduction in their ability to sequester fluorescein and an increased staining with propidium iodide, two effects that are consistent with cell death, were also evident after Aβ 1–40 treatment (Figs. 1C and D). Exposure of neurons to vehicle or the reversed peptide (Aβ 40–1) did not cause any significant degenerative change (Figs. 1C and D). Finally, another cell-death-related effect was the induction of the proapoptotic Bax 40 h after Aβ 1–40 treatment (Fig. 1E).

By using oligonucleotide microarrays we monitored mRNA expression profiles in cortical neurons exposed for 24 or 48 h to vehicle, 20 μM Aβ 1–40, or 20 μM Aβ 40–1. Among the 8740 genes interrogated by the microarrays, 241 genes showed significant changes following Aβ 1–40 but not Aβ 40–1 treatment. Among these, 71 were down-regulated and 34 up-regulated at 24 h, whereas 80 genes were down-regulated and 59 were up-regulated at 48 h.

Although our data represented the average gene expression from three separate microarray analyses, we confirmed the reliability of the array data by quantitatively validating the differential expression of five genes under each of the six experimental conditions using real-time quantitative reverse transcription–polymerase chain reaction (RT-PCR) (Table 1). Remarkably, the pattern of gene expression from sample to sample observed by microarrays closely paralleled the pattern observed using real-time RT-PCR. The mean±STD of the correlation coefficients between the two profiles is 0.97±0.01 (Table 1).

A hierarchical clustering method was used to group genes differentially expressed after exposure to Aβ on the basis of similarity in their expression patterns (Fig. 2). Genes segregating into four major branches of the dendrogram were assigned to four clusters. Clusters 1 and 2 represent those genes that were up-regulated, whereas clusters 3 and 4 differentiate those genes that were down-regulated after exposure to Aβ.

Among the 241 genes differentially expressed in cortical neurons after exposure to Aβ, 190 were assigned to functional categories and subcategories (Fig. 3) and to subcellular compartments (Fig. 4) based on their translated products.

Discussion

Some of the genes implicated in the present study have been previously associated with neuronal cell death, whereas others

Table 1
Validation of microarray data by real-time quantitative PCR

Name	GenBank	Control 24 h	βAP 40–1 24 h	βAP 1–40 24 h	Control 48 h	βAP 40–1 48 h	βAP 1–40 48 h	Corr. Coeff.	Forward primer	Reverse primer
Gastric inhibitory polypeptide receptor	L19660	563±34 1.22±0.09	134±21 0.37±0.03	280±27 0.50±0.05	1210±131 2.44±0.15	891±76 1.83±0.20	320±25 0.78±0.06	0.99	AGCTGAGGACTCGACAGATG	CACTGTTCCTGAAGGCTGAG
Glucose-dependent insulinotropic peptide	M92916	210±15 0.91±0.08	195±23 1.00±0.14	202±18 1.03±0.09	231±17 1.00±0.07	250±31 1.20±0.06	62±11 0.32±0.04	0.97	CCACAGAATCCAACAGGAAG	AGAGTGAGGAGCCAGGAGAC
EST	AA892259	1376±121 1.21±0.07	779±61 0.46±0.03	1450±110 0.93±0.05	1511±122 1.16±0.06	1543±146 1.08±0.90	258±28 0.21±0.01	0.95	GTACTCTGTGAGGCAGGTGG	GGCTCAGTGCAGTTAGAGGA
EST	AI639525	691±58 1.32±0.07	720±42 1.16±0.17	317±28 0.49±0.03	1119±108 2.70±0.15	481±41 0.84±0.06	522±43 0.84±0.08	0.97	ACCAGTCAAGACATTGCTCC	CAGATACACGGTACAGGCAG
Olf-1/EBF-associated Zn-finger protein Roaz	U92564	44±3.3 0.92±0.05	52±6.1 0.96±0.15	12±0.92 0.27±0.02	39±3.2 1.04±0.19	56±4.2 1.36±0.14	113±17 1.91±0.25	0.95	TCTGCTTCCTGCTACACCTC	CTCTGTGGTCTTCTCGGTGA

Quantitative-PCR, mean copies/100 pg RT-RNA±STD; microarray data, mean normalized values±STD.

provide a significant number of unique and novel entry points. In many cases, genes with common biological functions or in the same metabolic pathway showed coordinated expression. For this reason, in the following paragraphs we will discuss some of the genes implicated by microarray analysis, giving more emphasis to functional clusters of coregulated genes and pathways.

Apoptosis regulators

Among those genes that are conventionally designated as apoptosis regulators, we observed the differential expression of Bcl-2 and BTB (POZ) domain-containing 14B, two genes involved in triggering apoptosis [14]; annexin A5, which binds to cells undergoing programmed cell death [15]; and death-associated protein [16].

Cell-to-cell contact

A large number of genes encoding extracellular matrix proteins were differentially expressed in apoptotic cortical neurons and may reflect an extensive morphological remodeling that neurons undergo when exposed to β-amyloid. Some of the up-regulated genes (biglycan, tenascin-C, and lysyl oxidase) have been previously linked to neuronal survival, repair processes, and peripheral nerve regeneration [17,18], whereas those down-regulated (syndecan-4, neogenin, chondroitin sulfate proteoglycan 2, collagen type V α1, and integrin β4) were previously involved in apoptosis [19,20], neurological diseases, and plasticity [21,22].

Cellular cycle

The increase in growth arrest-specific 5 and growth arrest and DNA-damage-inducible 45α (gadd45) is consistent with the role of these gene families (gas and gadd) in the regulation of the cell death program and DNA repair [23,24]. The up-regulation of gadd45 has been previously reported in neurons exposed to Aβ [25] and in brain tissue obtained from patients suffering from Alzheimer disease [24]. Additionally, cell lines overexpressing this protein confer resistance to apoptosis [24]. Taken together, therefore, these data substantiate a role for gadd45 in the response (damage/recovery) to Aβ neurotoxicity.

Metabolism

Glutathione metabolism

Differential expression of genes involved in glutathione metabolism (glutathione reductase, glutamate-cysteine ligase, and 5-oxoprolinase) is concordant with the hypothesis of an altered glutathione-dependent antioxidant capacity during apoptosis and neurodegeneration [26–28].

Heme metabolism

Altered expression of two genes, heme oxygenase-1 and hydroxymethylbilane synthase, in cortical neurons exposed to Aβ confirms previous findings showing a relationship between heme turnover and neurodegeneration [29–31]. Increase in

heme oxygenase-1, in particular, has been also found in Alzheimer disease [32].

Fatty acid and lipid metabolism

The increased expression of carnitine palmitoyltransferase 1b, an enzyme involved in β-oxidation of fatty acid, may reflect an increased demand for energy production and parallels similar changes we have previously observed in cerebellar granule cells undergoing apoptosis following serum and potassium deprivation [13].

In neurons exposed to Aβ we also observed the increased expression of three genes involved in lipid metabolism (phospholipid scramblase 3, sialyltransferase 4B, and apolipoprotein L3) that have been previously linked to neurodegeneration and Alzheimer disease [33–35]. Conversely, down-regulation of carboxyl ester lipase and carboxylesterase 1 is concordant with their protecting role [36,37].

Metal binding

Increased expression of metallothionein 1a is consistent with its ability to protect neurons in CNS injury and repair [38].

Protein folding

Heat shock proteins act as molecular chaperones by assisting other proteins in folding, transport, and assembly into complexes. Differential expression of heat shock proteins constitutes a fundamental protective mechanism that allow cells to escape the otherwise inevitable engagement of cell death [39]. Consistent with this hypothesis, we observed altered expression of crystallin βA4, crystallin γE, α-crystallin-related B6, and DnaJ homolog, which are known to regulate apoptosis and underlie the pathogenesis of degenerative diseases [40,41].

Sterol biosynthesis

Altered expression of genes involved in sterol biosynthesis, such as mevalonate kinase, may reflect alteration of cholesterol homeostasis that has been related to the pathogenesis of Alzheimer disease [42].

Thyroid hormone

Intracellular concentrations of the thyroid hormones T4 and T3 are influenced by the activity of thyroxine deiodinases (TD). TD-III, in particular, catalyzes the degradation of both T4 and T3 to inactive derivatives. The observed increase in TD-III in cortical neurons exposed to Aβ may facilitate cell death by influencing the intracellular rates of T4-to-T3 conversion and confirms our previous findings in apoptotic cerebellar granule cells [13,43].

Signal transduction

G-protein-coupled receptors

Differential expression of several genes encoding G-protein-coupled receptors was observed in cortical neurons following Aβ treatment. Among these are the adrenergic receptor α2c and five different olfactory receptors that have been previously associated with programmed cell death [44,13].

Intracellular signaling

Decreased expression of inositol 1,4,5-triphosphate receptor 1 has been reported in several neurodegenerative diseases, including Alzheimer disease, Huntington chorea, and ischemia [45–47], all conditions in which neuronal loss occurs.

Differential expression of various kinases that are known to modulate cellular growth and cell death was observed in neurons exposed to Aβ. Reduced expression of PKC-γ, for example, confirms its protective role against cell death [48]. Increased expression of MAP kinase-activated protein kinase 2 has been previously reported following Aβ overproduction [49]. Decreased expression of GTP cyclohydrolase I has been previously linked to Alzheimer and Parkinson disease [50,51].

Reduced expression of afamin is in agreement with its protective role against Aβ-induced cell death of cortical neurons [52].

Ion homeostasis and ligand-gated ion channels

We observed the differential expression of a number of genes encoding proteins involved with potassium (Kctd13, Kcnj4), sodium (Scn11a), calcium (Cacnb1, Cacnb3, Chrna9, P2rx3), and chloride (Glra2, Clcn5) transport. As previously indicated, alterations in the transmembrane gradients of these ions may influence programmed cell death [53].

Secreted peptides and their receptors

Four genes (leukemia-inhibitory factor, secreted phosphoprotein 1, transforming growth factor-β receptor 3, and noggin) encoding key proteins implicated in the transforming growth factor-β (TGF-β) signaling pathway were differentially expressed in neurons exposed to Aβ. Activity of these proteins [54–59] and the TGF-β signaling pathway [60–64] is known to exert neuroprotective effects and prevent cell death.

Decreased expression of somatostatin has been previously related to Alzheimer disease [65]. Reduced expression of neurotrophin-5 and neurotrophic tyrosine kinase receptor type 3 is consistent with their neuroprotective role [66,54].

Increased expression of lipocalin 2 is in agreement with other studies showing its proapoptotic effect [67–69].

The coordinated reduction of glucose-dependent insulinotropic peptide (GIP) and its receptor mRNAs was observed in cortical neurons 48 h after Aβ treatment. Although mitogenic and antiapoptotic signaling of GIP has been demonstrated only in pancreatic β cells [70], their wide expression in brain [71,72] may support a neuroprotective role.

Transcription or translation regulation

Among transcription factors we observed the altered expression of USF1 [73], Max [74], Ciao1 [75], Mdm2 [76], and Nr3c2 [77], which have been previously involved in apoptotic cell death in the nervous system.

Conclusions

While demonstrating the utility of a cDNA-microarray system as a means of dissecting the multigenic program

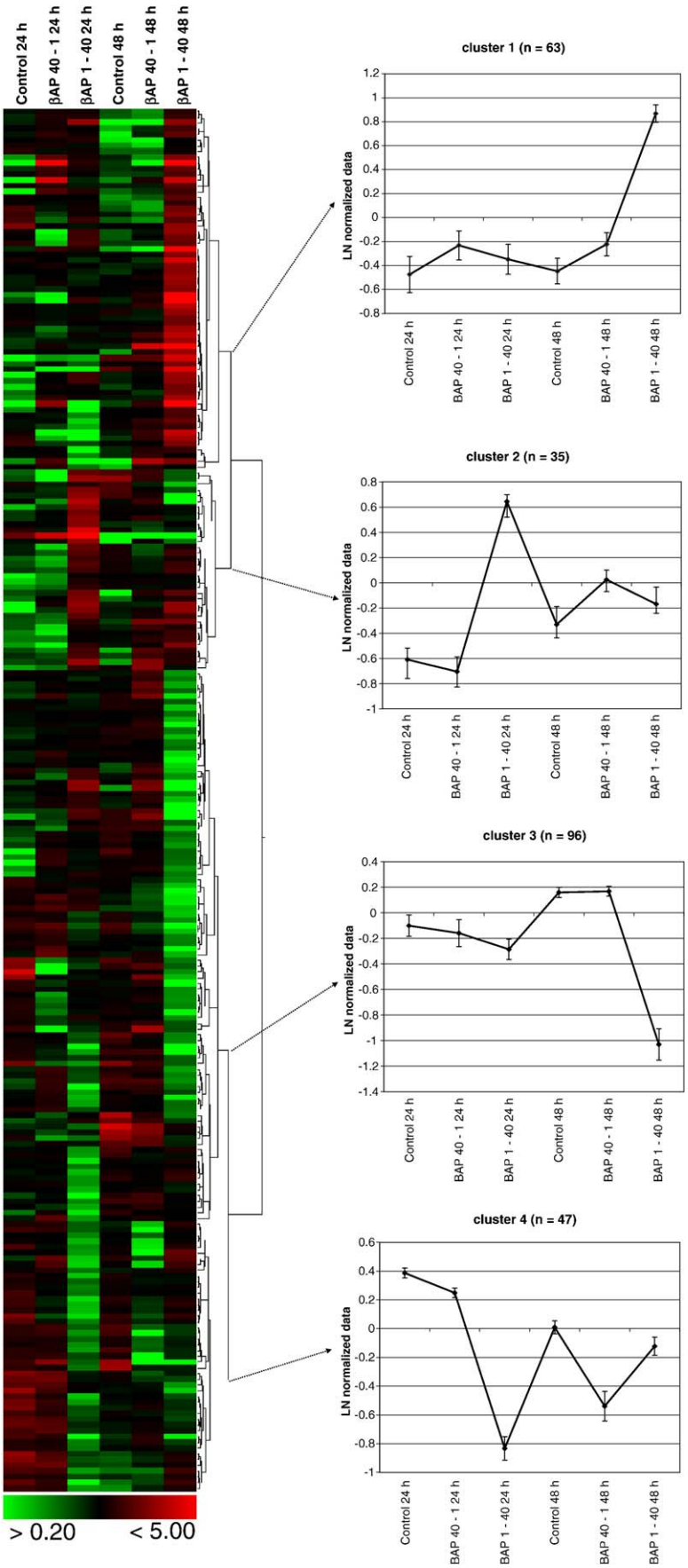
Control 24 h
βAP 40 - 1 24 h
βAP 1 - 40 24 h
Control 48 h
βAP 40 - 1 48 h
βAP 1 - 40 48 h
> 0.20
< 5.00
cluster 1 (n = 63)
cluster 2 (n = 35)
cluster 3 (n = 96)
cluster 4 (n = 47)
LN normalized data
Control 24 h
BAP 40 - 1 24 h
BAP 1 - 40 24 h
Control 48 h
BAP 40 - 1 48 h
BAP 1 - 40 48 h

underlying Aβ-induced cell death, the data presented represent just a glimpse of this complex phenomenon. It should be emphasized that the microarray provides estimates of changes in mRNA levels that cannot be correlated with the amount and function of the gene products. Translation and posttranslational modifications of many gene products and protein turnover have dramatic effects on function, and these cannot be inferred from expression analysis alone.

Most of the gene expression changes observed in the present study, having a larger or smaller specific weight, may contribute to the development of life or death. The exact role and functional relationships of the genes implicated are presumably those we cannot yet recognize. Gene expression profiles unlock virtually unexplored frontiers and we will learn as we explore them. Systematic characterization of expression patterns associated with neuronal cell death under different pathophysiological conditions and in distinct temporal domains will provide a framework for interpreting the biological significance of the expression patterns observed in the present study. We have just begun such a challenging task by characterizing gene expression profiles in cerebellar granule cells following serum and potassium deprivation [13]. Among the genes implicated in this model of neuronal cell death, 33 were in common with those differentially expressed in cortical neurons following Aβ exposure (shown in bold in Fig. 3 and in Supplementary, Table 1). Although preliminary, these data suggest the existence of both common and diverse mechanisms responsible for neuronal cell death. Knowledge of the mechanisms and pathways that are associated with neuronal cell death and are aberrant in pathological conditions will pave the way to new and effective therapeutic approaches.

Materials and methods

Materials

All the substances were obtained from Sigma unless otherwise specified. Aβ 1–40 and Aβ 40–1 were obtained from Bachem (Bachem, Torrance, CA, USA). Peptides were dissolved in water at a 1 mM concentration; 3 days before the experiment they were diluted with phosphate-buffered saline (PBS) at 500 mM and kept at 37°C until added to the cultures.

Animals

Pregnant Wistar rats (Charles River, Lecco, Italy) were sacrificed by exposure to CO_2. Experiments were approved in advance by the Animal Care and Use Committee and are consistent with the European Communities Council Directive of November 24, 1986 (86/609/EEC).

Neuronal cultures

Neurons were prepared from 17-day-old fetuses, according to a previously published protocol [78]. In brief, the fetuses were decapitated, and the brains were dissected and placed in PBS containing 4.5 g/L glucose. Hemispheres were separated, and meninges were carefully removed. Cortical tissues were freed from subcortical structures and cut into small fragments. Tissues were incubated with papain activated with cysteine for 10 min at 37°C. Papain was neutralized with a solution of ovomucoid and bovine serum albumin. Finally, tissues were mechanically dissociated until a single-cell suspension was obtained. Cells were plated in poly-D-lysine-coated 3.5-cm-diameter petri dishes, 48-multiwell plates, or tissue culture flasks. After 48 h, 1 μM cytosine arabinoside was added to the cells to inhibit glial cell growth.

Purity of cultures

To determine the purity of neuronal culture, we performed indirect immunofluorescence for a neuron-specific marker (neuron-specific nuclear protein, NeuN) and an astrocyte-specific marker (glial fibrillary acidic protein, GFAP) using a method previously described [79]. Primary antibodies against NeuN (1:250; Chemicon International, Temecula, CA, USA) were raised in mouse and diluted 1:250, whereas primary antibodies against GFAP (1:500; Chemicon International) were raised in rabbit. Secondary antibodies used were Texas red-conjugated anti-mouse (1:200; Santa Cruz Biotechnology, Heidelberg, Germany) and FITC-conjugated anti-rabbit (1:200; Chemicon International).

Viability assessment

Viability of cortical neurons was assessed with a propidium iodide exclusion test and fluorescein diacetate incorporation assessment, according to a previously published protocol [80]. Rat cortical neurons seeded on 3.5-cm-diameter dishes were treated, washed with PBS, and incubated with a PBS solution containing 36 μM fluorescein diacetate and 7 μM propidium iodide for 3 min at room temperature. Cell viability was assessed by counting 100 cells per microscope field (using a 20× lens) for the number of fluorescein-labeled neurons versus propidium-positive cells. Experiments were conducted in duplicate and repeated at least three times. Statistical validity was assessed by ANOVA followed by a post hoc test.

Analysis of apoptotic neuronal death

The typical morphological features of apoptotic degeneration were analyzed by fluorescence microscopy with the nuclear dye Hoechst 33258 as previously described [81]. Forty-eight hours after Aβ 1–40 exposure, neuronal cultures were washed once in PBS and then fixed in 2% paraformaldehyde. Apoptotic death was quantified after staining the cultures with the fluorescent chromatin dye Hoechst 33258 (0.4 μg/ml). Both normal and apoptotic neurons were scored from three random fields per dish in three individual dishes under an Olympus fluorescence microscope with a 60× magnification objective. Normal neurons exhibited a regularly dispersed chromatin, whereas apoptotic neurons were recognized by nuclear condensation and/or fragmented chromatin. To examine apoptosis-related effects we measured the expression of the proapoptotic Bax [82] by Western blot analysis as previously described [83].

Microarray analysis

Total RNA extracted from three biological replicates for each experimental condition (control 24 h, Aβ 40–1 24 h, Aβ 1–40 24 h, control 48 h, Aβ 40–1 48 h, Aβ 1–40 48 h) was reverse transcribed, biotinylated, and hybridized to Affymetrix GeneChip Rat Genome U34A arrays with the protocol outlined in the GeneChip Expression Analysis Technical Manual (Affymetrix, Santa Clara, CA, USA). The arrays were washed and stained by using a fluidics system with streptavidin–

Fig. 2. Genes differentially expressed in cortical neurons after Aβ treatment. A hierarchical clustering algorithm (Pearson correlation) was used to order 241 genes differentially expressed 24 and/or 48 h after Aβ treatment. Genes were arranged in a dendrogram in which the pattern and length of the branches reflect the relatedness of the expression levels under four different experimental conditions. Data are presented in a matrix format: each row represents a single gene and each column an experimental condition. The averaged normalized intensity from two replicates is represented by the color of the corresponding cell in the matrix. Green, black, and red cells, respectively, represent transcript levels below, equal to, or above the median abundance across all conditions. Color intensity reflects the magnitude of the deviation from the median (see scale at the bottom). The graphs on the right of the dendrogram represent the averaged natural log of normalized data±SEM of the genes in four major clusters. (For interpretation of the references to colour in this figure legend, the reader is referred to the web version of this article.)

A

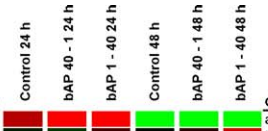

GenBank ID	Gene Title	Functional Category	Functional Subcategory
AF051895	annexin A5	Apoptosis regulator	
L14680	B-cell leukemia/lymphoma 2		
AF015911	BTB (POZ) domain containing 14B		
AI639136	death-associated protein		
X86178	alpha-2-glycoprotein 1, zinc	Cell to cell contact	
D10261	alpha-2-HS-glycoprotein		
AA859830	biglycan		
AF072892	chondroitin sulfate proteoglycan 2		
AA859757	collagen, type V, alpha 1		
X14323	Fc receptor, IgG, alpha chain transporter		
L07398	immunoglobulin rearranged gamma-chain mRNA variable (V) region		
U60096	integrin beta 4		
S77494	lysyl oxidase		
M22924	membrane-spanning 4-domains, subfamily A, member 2		
U48246	NEL-like 1		
U68726	neogenin		
AI044259	putative cell surface antigen		
M11071	**RT1 class I, CE12**		
AF074608	**RT1 class Ib, locus Aw2**		
D45240	RT1 class II, locus DOa		
M14656	secreted phosphoprotein 1		
U76836	similar to T-cell receptor alpha chain precursor V and C regions (TRA29)		
S61868	syndecan 4		
M18854	T-cell receptor beta-2 chain C region		
U09361	tenascin C		
U15550	tenascin C		
AB016425	thiopurine methyltransferase		
AI638971	thiopurine methyltransferase		
L32591	growth arrest and DNA-damage-inducible 45 alpha	Cellular cycle	
U77829	growth arrest specific 5		
M35270	**alanine-glyoxylate aminotransferase**	Metabolism	Amino acid metabolism
X06357	**alanine-glyoxylate aminotransferase**		
J03637	aldehyde dehydrogenase family 3, member A1		Carbohydrate metabolism
AI103396	cytochrome b, mitochondrial		Electron transport
J02657	cytochrome P450, subfamily IIC (mephenytoin 4-hydroxylase)		
J05031	isovaleryl coenzyme A dehydrogenase		
AF063302	**carnitine palmitoyltransferase 1b**		Fatty acid metabolism
AF067790	palmitoyl-protein thioesterase 2		
U70825	5-oxoprolinase (ATP-hydrolysing)		Glutathione metabolism
AI233261	glutamate cysteine ligase, modifier subunit		
AA893189	**glutathione reductase**		
M27726	brain glycogen phosphorylase		Glycogen metabolism
AI179610	heme oxygenase 1		Heme metabolism
X06827	hydroxymethylbilane synthase		
AA800319	apolipoprotein L3		Lipid metabolism
X16054	carboxyl ester lipase		
U10697	carboxylesterase 1		
U36772	glycerol-3-phosphate acyltransferase, mitochondrial		
AA800303	phospholipid scramblase 3		
AA859911	sialyltransferase 4B		
U38306	arylalkylamine N-acetyltransferase		Melatonin synthesis
M11794	**metallothionein 1a**		Metal binding
AF013247	crystallin, beta A4		Protein folding
M19357	crystallin, gamma E		
AI011998	DnaJ (Hsp40) homolog, subfamily B, member 9		
AI103838	heat shock protein, alpha-crystallin-related, B6		
AF043642	peptidylprolyl isomerase G		
AI639506	F-box only protein 30		Protein ubiquitylation
AA799593	ubiquitin-conjugating enzyme E2H		
AF017637	carboxypeptidase Z		Proteolysis
AA925246	cathepsin K		
S80379	chymotrypsin C (caldecrin)		
J04591	dipeptidylpeptidase 4		
S73583	glutamyl aminopeptidase		
S40669	proprotein convertase subtilisin/kexin type 2		
AI069990	tripeptidyl peptidase II		
U91561	pyridoxine 5'-phosphate oxidase		Pyridoxine synthesis
D17309	aldo-keto reductase family 1, member D1		Sterol biosynthesis
J02827	**branched chain ketoacid dehydrogenase E1, alpha polypeptide**		
M29472	mevalonate kinase		
S70803	START domain containing 3		
S81448	steroid 5 alpha-reductase 1		
U37138	steroid sulfatase		
L16995	sterol regulatory element binding factor 1		
U24282	**deiodinase, iodothyronine, type III**		Thyroid hormone
AA859827	uridine monophosphate kinase		Various
AA891242	myosin, light polypeptide 7, regulatory	Structural and cytoskeletal proteins	Cytoskeletal proteins
D88034	peptidyl arginine deiminase, type III		
AF031878	peripherin 1		
U59240	tropomodulin 2		
AA866465	**tropomyosin isoform 6**		
U72353	lamin B1		Nuclear proteins
U19614	**lamina-associated polypeptide 1B**		
U67139	discs, large homolog-associated protein 3	Synaptic protein	
AB007688	homer homolog 1		
AF102853	**membrane-associated guanylate kinase-interacting protein**		
AI146018	neurexin 1		
AA893634	coatomer protein complex, subunit zeta 2	Transport	Intracellular protein transport
AA799691	**K-Cl cotransporter KCC4**		Solute carrier
AF008439	solute carrier family 11		
AA859652	**solute carrier family 16 (monocarboxylic acid transporters), member 6**		
M13979	solute carrier family 2 (facilitated glucose transporter), member 1		
AJ223355	solute carrier family 25, member 10		
AA891700	transmembrane protein 1		

Fig. 3. Functional clustering of genes differentially expressed in cortical neurons after Aβ treatment. Genes whose translated products have a recognized function were clustered into different functional categories and subcategories. Shown in bold are those genes that are also differentially expressed in apoptotic cerebellar granule neurons following serum and potassium deprivation [13].

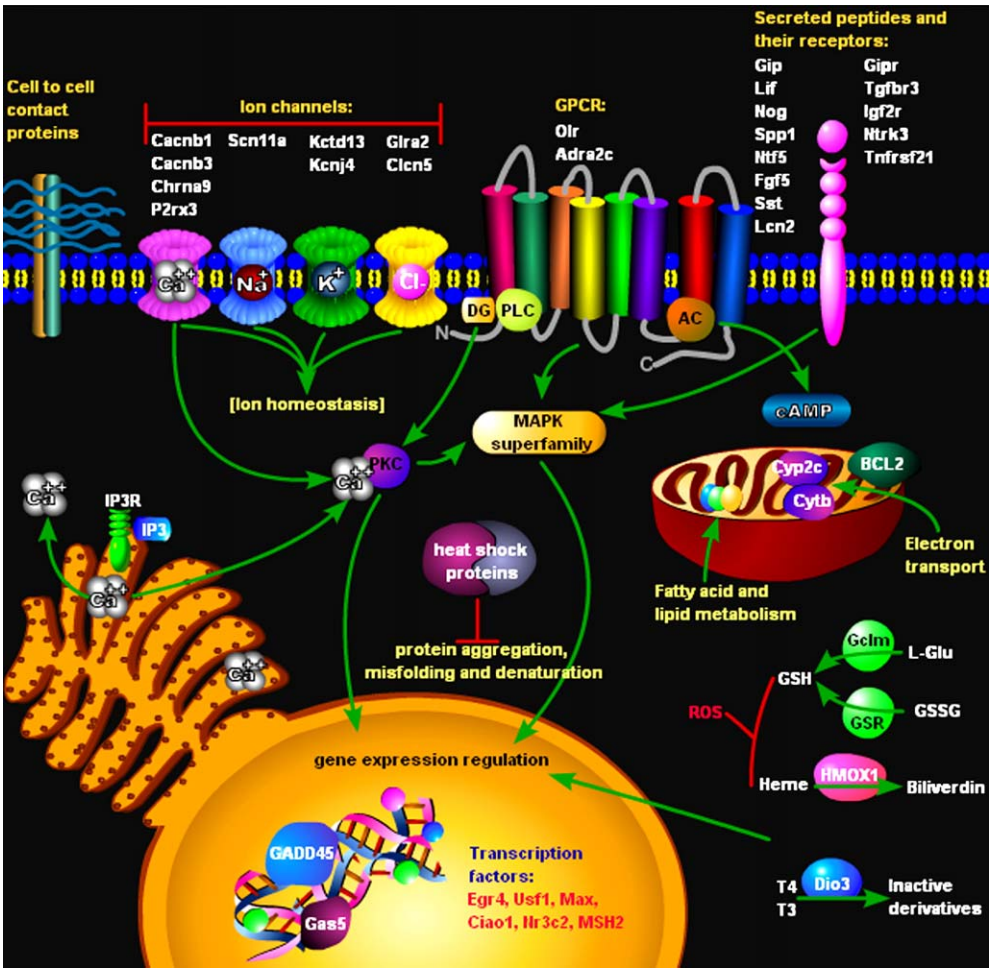

Fig. 4. Subcellular localization of proteins encoded by genes differentially expressed in cortical neurons after Aβ treatment. Some of the genes whose translated products have a recognized function and subcellular localization are represented in different functional groups and subcellular compartments. In the *plasma membrane* are cell-to-cell contact proteins; ion channels Cacnb1 (calcium channel, voltage-dependent, β1 subunit), Cacnb3 (calcium channel, voltage-dependent, β3 subunit), Chrna9 (cholinergic receptor, nicotinic, α polypeptide 9), Clcn5 (chloride channel 5), Glra2 (glycine receptor, α2 subunit), Kcnj4 (potassium inwardly rectifying channel, subfamily J, member 4), Kctd13 (potassium channel tetramerization domain-containing 13), P2rx3 (purinergic receptor P2X, ligand-gated ion channel, 3), Scn11a (sodium channel, voltage-gated, type11, α polypeptide); G-protein-coupled receptors (GPCR) Adra2c (adrenergic receptor, α2c), Olr (olfactory receptors 1346, 1346, 1504, 1530, 1696, 837); secreted peptides and their receptors Fgf5 (fibroblast growth factor 5), Gip (glucose-dependent insulinotropic peptide), Gipr (gastric inhibitory polypeptide receptor), Igf2r (insulin-like growth factor 2 receptor), Lcn2 (lipocalin 2), Lif (leukemia-inhibitory factor), Nog (noggin), Ntf5 (neurotrophin 5), Ntrk3 (neurotrophic tyrosine kinase, receptor, type 3), Sst (somatostatin), Tgfbr3 (transforming growth factor, β receptor 3), Tnfrsf21 (TNFR-related death receptor 6); DG (diacylglycerol); PLC (phospholipase-C); and AC (adenylate cyclase). In the *endoplasmic reticulum* is IP3 (inositol 1,4,5-triphosphate receptor 1). In the *cytosol* are PKC (protein kinase Cγ); heat shock proteins (crystallin βA4; crystallin γE; DnaJ, Hsp40, homolog, subfamily B, member 9; heat shock protein α-crystallin-related B6; peptidylprolyl isomerase G); MAPK superfamily (MAP kinase-activated protein kinase 2, mitogen-activated protein kinase 7); ROS (reactive oxygen species); glutathione metabolism proteins Gclm (glutamate cysteine ligase, modifier subunit), GSH (reduced glutathione), GSSG (oxidized glutathione), Gsr (glutathione reductase) L-Glu (L-glutamate); Hmox1 (heme oxygenase 1); thyroid hormone metabolism proteins Dio3 (deiodinase, iodothyronine, type III), T4 (thyroxine), and T3 (triiodothyronine). In the *mitochondria* are fatty acid metabolism proteins carnitine palmitoyltransferase 1b, palmitoyl-protein thioesterase 2; lipid metabolism proteins apolipoprotein L3 carboxyl ester lipase, carboxylesterase 1, glycerol-3-phosphate acyltransferase (mitochondrial), phospholipid scramblase 3, sialyltransferase 4B; electron transport proteins Cytb (cytochrome *b,* mitochondrial), Cyp2c (cytochrome P450, subfamily IIC); and Bcl2 (B-cell leukemia/lymphoma 2). In the *nucleus* are cell cycle proteins Gadd45a (growth arrest and DNA-damage-inducible 45α), Gas5 (growth arrest-specific 5); transcription factors Egr4 (early growth response 4), Ciao1 (WD40 protein Ciao1), Max, Msh2 (mutS homolog 2), Nr3c2 (nuclear receptor subfamily 3, group C, member 2), and Usf1 (upstream transcription factor 1).

phycoerythrin (Molecular Probes, Eugene, OR, USA), amplified with biotinylated anti-streptavidin antibody (Vector Laboratories, Burlingame, CA, USA), and then scanned with a GeneArray Scanner (Affymetrix). To determine the quality of labeled targets prior to analysis on GeneChip Rat Genome U34A arrays, each sample was hybridized to one GeneChip Test3 array. The image data were analyzed by the MicroArray Suite 4.0 gene expression analysis program (Affymetrix). Normalization, filtering, and cluster analysis of the data were performed with the GeneSpring 7.2 software (Silicon Genetics, Redwood City, CA, USA). Each gene was normalized to itself by making a synthetic positive control for that gene and dividing all measurements for that gene by this positive control. This synthetic control was the median of the gene's expression values over all the samples. Average difference values of less than 0 represent probe sets for which the intensity of the mismatched probe was on average greater than that of the perfect matched probe and, thus, the probe set was performing poorly. For this reason, normalized values below 0 were set to 0.01. To test for statistically significant changes in signal intensity, genes with an average change greater than twofold were screened by the Mann–Whitney *U* test (p value <0.05) using the Benjamini and Hochberg False Discovery Rate procedure to adjust for multiple comparisons. A complete list of differentially expressed genes is available online as Supplementary Table 2 and at http://web.tiscali.it/sebastiano_cavallaro.

Real-time quantitative RT-PCR

Following extraction, total RNA samples (three/experimental condition) were reverse transcribed with oligo(dT)$_{12–18}$ and SuperScript II RNase H$^-$ reverse transcriptase (Invitrogen Life Technologies, Carlsbad, CA, USA). Aliquots of cDNA (0.1 and 0.2 μg) and known amounts of external standard (purified PCR product, 10^2 to 10^8 copies) were amplified in parallel reactions using primers indicated in Table 1. To control for the integrity of RNA and for differences attributable to errors in experimental manipulation, mRNA levels of mouse ribosomal S18 and phosphoglycerate kinase 1 were measured in similar reactions. Each PCR (final volume 20 μl) contained 0.5 μM primers, 2.5 mM Mg^{2+}, and 1× DNA SYBR green master mix (Roche Molecular Biochemicals, Mannheim, Germany). PCR amplifications were performed with a Light-Cycler (Roche Molecular Biochemicals) using the following cycle program: (i) denaturation of cDNA (1 cycle, 95°C for 1 min), (ii) amplification (40 cycles, 95°C for 0 s, 57°C for 5 s, 72°C for 10 s), (iii) melting curve analysis (1 cycle, 95°C for 0 s, 67°C for 10 s, 95°C for 0 s), (iv) cooling (1 cycle, 40°C for 3 min). Temperature transition rate was 20°C/s except for the third segment of the melting curve analysis, for which it was 0.2°C/s. Fluorimeter gain value was 7. Real-time detection of fluorimetric intensity of SYBR Green I, indicating the amount of PCR product formed, was measured at the end of each elongation phase. Quantification was performed by comparing the fluorescence of PCR products of unknown concentration with the fluorescence of the external standards. For this analysis, fluorescence values measured in the log-linear phase of amplification were considered using the second derivative maximum method of the Light-Cycler data analysis software (Roche Molecular Biochemicals). Specificity of PCR products obtained was characterized by melting curve analysis followed by gel electrophoresis and DNA sequencing.

Acknowledgments

We gratefully acknowledge Alfia Corsino, Maria Patrizia D'Angelo, and Francesco Marino for their administrative and technical support. This work was partly sponsored by grants from the Italian Ministry of Health and the Italian Ministry of Education University and Research (DM 1105/255) to S.C.

Appendix A. Supplementary data

Supplementary data associated with this article can be found, in the online version, at doi:10.1016/j.ygeno.2006.06.007.

References

[1] R.W. Oppenheim, Cell death during development of the nervous system, Annu. Rev. Neurosci. 14 (1991) 453–501.
[2] J.W. Allen, B.A. Eldadah, A.I. Faden, Beta-amyloid-induced apoptosis of cerebellar granule cells and cortical neurons: exacerbation by selective inhibition of group I metabotropic glutamate receptors, Neuropharmacology 38 (1999) 1243–1252.
[3] A. Copani, et al., Activation of metabotropic glutamate receptors protects cultured neurons against apoptosis induced by beta-amyloid peptide, Mol. Pharmacol. 47 (1995) 890–897.
[4] A. Copani, et al., Mitotic signaling by beta-amyloid causes neuronal death, FASEB J. 13 (1999) 2225–2234.
[5] S. Estus, et al., Aggregated amyloid-beta protein induces cortical neuronal apoptosis and concomitant "apoptotic" pattern of gene induction, J. Neurosci. 17 (1997) 7736–7745.
[6] G. Forloni, et al., Apoptosis mediated neurotoxicity induced by chronic application of beta amyloid fragment 25–35, NeuroReport 4 (1993) 523–526.
[7] M. Gschwind, G. Huber, Apoptotic cell death induced by beta-amyloid 1–42 peptide is cell type dependent, J. Neurochem. 65 (1995) 292–300.
[8] D.T. Loo, et al., Apoptosis is induced by beta-amyloid in cultured central nervous system neurons, Proc. Natl. Acad. Sci. U. S. A. 90 (1993) 7951–7955.
[9] J.J. Miguel-Hidalgo, R. Cacabelos, Beta-amyloid(1–40)-induced neurodegeneration in the rat hippocampal neurons of the CA1 subfield, Acta Neuropathol. (Berlin) 95 (1998) 455–465.
[10] C. Pereira, E. Ferreiro, S.M. Cardoso, C.R. de Oliveira, Cell degeneration induced by amyloid-beta peptides: implications for Alzheimer's disease, J. Mol. Neurosci. 23 (2004) 97–104.
[11] C. Behl, J.B. Davis, F.G. Klier, D. Schubert, Amyloid beta peptide induces necrosis rather than apoptosis, Brain Res. 645 (1994) 253–264.
[12] T. Pillot, et al., The nonfibrillar amyloid beta-peptide induces apoptotic neuronal cell death: involvement of its C-terminal fusogenic domain, J. Neurochem. 73 (1999) 1626–1634.
[13] S. Cavallaro, et al., Gene expression profiles of apoptotic neurons, Genomics 84 (2004) 485–496.
[14] L. Korutla, J.H. Neustadter, K.M. Fournier, S.A. Mackler, NAC1, a POZ/BTB protein present in the adult mammalian brain, triggers apoptosis after adenovirus-mediated overexpression in PC-12 cells, Neurosci. Res. 46 (2003) 33–39.
[15] B.L. Kietselaer, L. Hofstra, E.A. Dumont, C.P. Reutelingsperger, G.A. Heidendal, The role of labeled Annexin A5 in imaging of programmed cell death: from animal to clinical imaging, Q. J. Nucl. Med. 47 (2003) 349–361.
[16] G. Shohat, T. Spivak-Kroizman, M. Eisenstein, A. Kimchi, The regulation of death-associated protein (DAP) kinase in apoptosis, Eur. Cytokine Network 13 (2002) 398–400.
[17] J. Kappler, et al., Chondroitin/dermatan sulphate promotes the survival of neurons from rat embryonic neocortex, Eur. J. Neurosci. 9 (1997) 306–318.
[18] T. Hirayama, H. Sugino, T. Yagi, Somatic mutations of synaptic cadherin (CNR family) transcripts in the nervous system, Genes Cells 6 (2001) 151–164.
[19] M.A. Ferrari do Outeiro-Bernstein, et al., A recombinant NH(2)-terminal heparin-binding domain of the adhesive glycoprotein, thrombospondin-1, promotes endothelial tube formation and cell survival: a possible role for syndecan-4 proteoglycan, Matrix Biol. 21 (2002) 311–324.
[20] E. Matsunaga, et al., RGM and its receptor neogenin regulate neuronal survival, Nat. Cell Biol. 6 (2004) 749–755.
[21] J.M. Lemire, et al., Versican/PG-M isoforms in vascular smooth muscle cells, Arterioscler. Thromb. Vasc. Biol. 19 (1999) 1630–1639.
[22] Y. Kiuchi, Y. Isobe, K. Fukushima, Type IV collagen prevents amyloid beta-protein fibril formation, Life Sci. 70 (2002) 1555–1564.
[23] R. Hass, Retrodifferentiation and cell death, Crit. Rev. Oncog. 5 (1994) 359–371.
[24] R. Torp, J.H. Su, G. Deng, C.W. Cotman, GADD45 is induced in Alzheimer's disease and protects against apoptosis in vitro, Neurobiol. Dis. 5 (1998) 245–252.
[25] D. Santiard-Baron, et al., Identification of β-amyloid-responsive genes by RNA differential display: early induction of a DNA damage-inducible gene, gadd45, Exp. Neurol. 158 (1999) 206–213.
[26] C.C. Franklin, et al., Caspase-3-dependent cleavage of the glutamate-l-cysteine ligase catalytic subunit during apoptotic cell death, Am. J. Pathol. 160 (2002) 1887–1894.
[27] V. Lievre, et al., Intracellular generation of free radicals and modifications of detoxifying enzymes in cultured neurons from the developing rat forebrain in response to transient hypoxia, Neuroscience 105 (2001) 287–297.
[28] G. Wu, Y.Z. Fang, S. Yang, J.R. Lupton, N.D. Turner, Glutathione metabolism and its implications for health, J. Nutr. 134 (2004) 489–492.
[29] J.Z. Guo, Q.X. Zhou, (The research into functions of heme oxygenase system in brain), Sheng Li Ke Xue Jin Zhan 33 (2002) 26–29.
[30] R.L. Lindberg, et al., Motor neuropathy in porphobilinogen deaminase-deficient mice imitates the peripheral neuropathy of human acute porphyria, J. Clin. Invest. 103 (1999) 1127–1134.
[31] R.L. Lindberg, et al., Porphobilinogen deaminase deficiency in mice causes a neuropathy resembling that of human hepatic porphyria, Nat. Genet. 12 (1996) 195–199.
[32] H.M. Schipper, Heme oxygenase expression in human central nervous system disorders, Free Radical Biol. Med. 37 (2004) 1995–2011.

[33] A. Csaszar, J. Kalman, C. Szalai, Z. Janka, L. Romics, Association of the apolipoprotein A-IV codon 360 mutation in patients with Alzheimer's disease, Neurosci. Lett. 230 (1997) 151–154.
[34] R. Gander, et al., Molecular characterization of rabbit phospholipid transfer protein: choroid plexus and ependyma synthesize high levels of phospholipid transfer protein, J. Lipid Res. 43 (2002) 636–645.
[35] H. Kawai, et al., Mice expressing only monosialoganglioside GM3 exhibit lethal audiogenic seizures, J. Biol. Chem. 276 (2001) 6885–6888.
[36] D.Y. Hui, P.N. Howles, Carboxyl ester lipase: structure–function relationship and physiological role in lipoprotein metabolism and atherosclerosis, J. Lipid Res. 43 (2002) 2017–2030.
[37] T. Yamada, N. Kawaguchi, M. Hosokawa, T. Satoh, Localization of an isoform of carboxylesterase in rat brain differs from that in human brain, Brain Res. 674 (1995) 175–179.
[38] R.S. Chung, A.K. West, A role for extracellular metallothioneins in CNS injury and repair, Neuroscience 123 (2004) 595–599.
[39] H.M. Beere, "The stress of dying": the role of heat shock proteins in the regulation of apoptosis, J. Cell Sci. 117 (2004) 2641–2651.
[40] M.C. Kamradt, F. Chen, V.L. Cryns, The small heat shock protein alpha B-crystallin negatively regulates cytochrome c- and caspase-8-dependent activation of caspase-3 by inhibiting its autoproteolytic maturation, J. Biol. Chem. 276 (2001) 16059–16063.
[41] K.J. Lee, et al., Induction of molecular chaperones in carbon tetrachloride-treated rat liver: implications in protection against liver damage, Cell Stress Chaperones 9 (2004) 58–68.
[42] K. Sambamurti, et al., Cholesterol and Alzheimer's disease: clinical and experimental models suggest interactions of different genetic, dietary and environmental risk factors, Curr. Drug Targets 5 (2004) 517–528.
[43] Q. Xiao, V.M. Nikodem, Apoptosis in the developing cerebellum of the thyroid hormone deficient rat, Front. Biosci. 3 (1998) A52–A57.
[44] R.X. Wang, L.E. Limbird, Distribution of mRNA encoding three alpha 2-adrenergic receptor subtypes in the developing mouse embryo suggests a role for the alpha 2A subtype in apoptosis, Mol. Pharmacol. 52 (1997) 1071–1080.
[45] L.S. Haug, S.I. Walaas, A.C. Ostvold, Degradation of the type I inositol 1,4,5-trisphosphate receptor by caspase-3 in SH-SY5Y neuroblastoma cells undergoing apoptosis, J. Neurochem. 75 (2000) 1852–1861.
[46] J. Oberdorf, M.L. Vallano, R.J. Wojcikiewicz, Expression and regulation of types I and II inositol 1,4,5-trisphosphate receptors in rat cerebellar granule cell preparations, J. Neurochem. 69 (1997) 1897–1903.
[47] H. Tsubokawa, et al., Inositol 1,3,4,5-tetrakisphosphate as a mediator of neuronal death in ischemic hippocampus, Neuroscience 59 (1994) 291–297.
[48] A. Lombet, et al., Resistance to induced apoptosis in the human neuroblastoma cell line SK-N-SH in relation to neuronal differentiation: role of Bcl-2 protein family, Eur. J. Biochem. 268 (2001) 1352–1362.
[49] C. Song, G. Perides, D. Wang, Y.F. Liu, Beta-amyloid peptide induces formation of actin stress fibers through p38 mitogen-activated protein kinase, J. Neurochem. 83 (2002) 828–836.
[50] U.J. Kang, Potential of gene therapy for Parkinson's disease: neurobiologic issues and new developments in gene transfer methodologies, Mov. Disord. 1 (1998) 59–72.
[51] B. Thony, G. Auerbach, N. Blau, Tetrahydrobiopterin biosynthesis, regeneration and functions, Biochem. J. 347 (Pt. 1) (2000) 1–16.
[52] M. Heiser, et al., Vitamin E binding protein afamin protects neuronal cells in vitro, J. Neural Transm. Suppl. (2002) 337–345.
[53] S.P. Yu, L.M. Canzoniero, D.W. Choi, Ion homeostasis and apoptosis, Curr. Opin. Cell Biol. 13 (2001) 405–411.
[54] C. Limatola, et al., The chemokine growth-related gene product beta protects rat cerebellar granule cells from apoptotic cell death through alpha-amino-3-hydroxy-5- methyl-4-isoxazolepropionate receptors, Proc. Natl. Acad. Sci. U. S. A. 97 (2000) 6197–6201.
[55] J.C. Hardwick, et al., Bone morphogenetic protein 2 is expressed by, and acts upon, mature epithelial cells in the colon, Gastroenterology 126 (2004) 111–121.
[56] A.R. Hallahan, et al., BMP-2 mediates retinoid-induced apoptosis in medulloblastoma cells through a paracrine effect, Nat. Med. 9 (2003) 1033–1038.
[57] M. Kiyono, M. Shibuya, Bone morphogenetic protein 4 mediates apoptosis of capillary endothelial cells during rat pupillary membrane regression, Mol. Cell. Biol. 23 (2003) 4627–4636.
[58] A.A. Sharov, et al., Noggin overexpression inhibits eyelid opening by altering epidermal apoptosis and differentiation, EMBO J. 22 (2003) 2992–3003.
[59] P.C. Mabie, M.F. Mehler, J.A. Kessler, Multiple roles of bone morphogenetic protein signaling in the regulation of cortical cell number and phenotype, J. Neurosci. 19 (1999) 7077–7088.
[60] N. Bye, M. Zieba, N.G. Wreford, N.R. Nichols, Resistance of the dentate gyrus to induced apoptosis during ageing is associated with increases in transforming growth factor-beta1 messenger RNA, Neuroscience 105 (2001) 853–862.
[61] H.P. Deigner, U. Haberkorn, R. Kinscherf, Apoptosis modulators in the therapy of neurodegenerative diseases, Expert Opin. Invest. Drugs 9 (2000) 747–764.
[62] N. Dunker, N. Schuster, K. Krieglstein, TGF-beta modulates programmed cell death in the retina of the developing chick embryo, Development 128 (2001) 1933–1942.
[63] K.C. Flanders, R.F. Ren, C.F. Lippa, Transforming growth factor-betas in neurodegenerative disease, Prog. Neurobiol. 54 (1998) 71–85.
[64] Y. Zhu, et al., Transforming growth factor-beta 1 increases Bad phosphorylation and protects neurons against damage, J. Neurosci. 22 (2002) 3898–3909.
[65] G. Bissette, B. Myers, Somatostatin in Alzheimer's disease and depression, Life Sci. 51 (1992) 1389–1410.
[66] C. Hock, K. Heese, C. Hulette, C. Rosenberg, U. Otten, Region-specific neurotrophin imbalances in Alzheimer disease: decreased levels of brain-derived neurotrophic factor and increased levels of nerve growth factor in hippocampus and cortical areas, Arch. Neurol. 57 (2000) 846–851.
[67] L.R. Devireddy, J.G. Teodoro, F.A. Richard, M.R. Green, Induction of apoptosis by a secreted lipocalin that is transcriptionally regulated by IL-3 deprivation, Science 293 (2001) 829–834.
[68] K. Kamezaki, et al., The lipocalin 24p3, which is an essential molecule in IL-3 withdrawal-induced apoptosis, is not involved in the G-CSF withdrawal-induced apoptosis, Eur. J. Haematol. 71 (2003) 412–417.
[69] Z. Tong, X. Wu, J.P. Kehrer, Increased expression of the lipocalin 24p3 as an apoptotic mechanism for MK886, Biochem. J. 372 (2003) 203–210.
[70] A. Trumper, K. Trumper, D. Horsch, Mechanisms of mitogenic and anti-apoptotic signaling by glucose-dependent insulinotropic polypeptide in beta(INS-1)-cells, J. Endocrinol. 174 (2002) 233–246.
[71] T.B. Usdin, E. Mezey, D.C. Button, M.J. Brownstein, T.I. Bonner, Gastric inhibitory polypeptide receptor, a member of the secretin–vasoactive intestinal peptide receptor family, is widely distributed in peripheral organs and the brain, Endocrinology 133 (1993) 2861–2870.
[72] Y. Yamada, Y. Seino, Physiology of GIP—A lesson from GIP receptor knockout mice, Horm. Metab. Res. 36 (2004) 771–774.
[73] A.S. Jaiswal, S. Narayan, Upstream stimulating factor-1 (USF1) and USF2 bind to and activate the promoter of the adenomatous polyposis coli (APC) tumor suppressor gene, J. Cell. Biochem. 81 (2001) 262–277.
[74] H. Petrs-Silva, F.G. de Freitas, R. Linden, L.B. Chiarini, Early nuclear exclusion of the transcription factor Max is associated with retinal ganglion cell death independent of caspase activity, J. Cell. Physiol. 198 (2004) 179–187.
[75] B.A. Joughin, B. Tidor, M.B. Yaffe, A computational method for the analysis and prediction of protein:phosphopeptide-binding sites, Protein Sci. 14 (2005) 131–139.
[76] Y. Tu, S.T. Hou, Z. Huang, G.S. Robertson, J.P. MacManus, Increased Mdm2 expression in rat brain after transient middle cerebral artery occlusion, J. Cereb. Blood Flow Metab. 18 (1998) 658–669.
[77] O.F. Almeida, et al., Subtle shifts in the ratio between pro- and antiapoptotic molecules after activation of corticosteroid receptors decide neuronal fate, FASEB J. 14 (2000) 779–790.
[78] M. Grimaldi, S. Cavallaro, Expression and coupling of PACAP/VIP receptors in cortical neurons and type I astrocytes, Ann. N. Y. Acad. Sci. 921 (2000) 312–316.

[79] V. D'Agata, M. Grimaldi, A. Pascale, S. Cavallaro, Regional and cellular expression of the parkin gene in the rat cerebral cortex, Eur. J. Neurosci. 12 (2000) 3583–3588.
[80] A. Favit, F. Nicoletti, U. Scapagnini, P.L. Canonico, Ubiquinone protects cultured neurons against spontaneous and excitotoxin-induced degeneration, J. Cereb. Blood Flow Metab. 12 (1992) 638–645.
[81] S. Cavallaro, et al., Pituitary adenylate cyclase activating polypeptide prevents apoptosis in cultured cerebellar granule neurons, Mol. Pharmacol. 50 (1996) 60–66.
[82] X. Yan, et al., Carbachol blocks beta-amyloid fragment 31–35-induced apoptosis in cultured cortical neurons, Brain Res. Bull. 51 (2000) 465–470.
[83] M. Calafiore, et al., Progenitor cells from the adult mouse brain acquire a neuronal phenotype in response to beta-amyloid, Neurobiol. Aging 27 (2006) 606–613.